https://doi.org/10.5194/acp-2021-683
Preprint. Discussion started: 5 October 2021

Atmospheric Chemistry and Physics Discussions

Estimation of Secondary $PM_{2.5}$ in China and the United States using a Multi-Tracer Approach

Haoran Zhang [1], Nan Li [1,*], Keqin Tang [1], Hong Liao [1,*], Chong Shi [2,3], Cheng Huang [4], Hongli Wang [4], Song Guo [5], Min Hu [5], Xinlei Ge [1], Mindong Chen [1], Zhenxin Liu [1], Huan Yu [6], Jianlin Hu [1]

[1] Jiangsu Key Laboratory of Atmospheric Environment Monitoring and Pollution Control, Jiangsu Collaborative Innovation Center of Atmospheric Environment and Equipment Technology, School of Environmental Science and Engineering, Nanjing University of Information Science & Technology, Nanjing, 210044, China

[2] National Institute for Environmental Studies，Center for Global Environmental Research，Tsukuba，Ibaraki，Japan

[3] Institute of Remote Sensing and Digital Earth, Chinese Academy of Sciences, Beijing, 100094, China

[4] State Environmental Protection Key Laboratory of Formation and Prevention of the Urban Air Pollution Complex, Shanghai Academy of Environmental Sciences, Shanghai, 200233, China

[5] College of Environmental Sciences and Engineering, Peking University, Beijing, 100871, China

[6] Department of Atmospheric Science, School of Environmental Studies, China University of Geosciences, Wuhan, 430074, China

[*] *Correspondence to:*

Nan Li, linan@nuist.edu.cn and Hong Liao, hongliao@nuist.edu.cn

https://doi.org/10.5194/acp-2021-683
Preprint. Discussion started: 5 October 2021

Atmospheric Chemistry and Physics Discussions

Abstract:

$PM_{2.5}$, generated via both direct emissions and secondary formations, can have varying environmental impacts due to different physical and chemical properties of its components. However, traditional methods to quantify different $PM_{2.5}$ components are often based on online observations or lab analyses, which are generally high economic cost and labor-intensive. In this study, we develop a new method, named multi-tracer estimation algorithm (MTEA), to identify the primary and secondary components from routine observation of $PM_{2.5}$. By comparing with the long-term and short-term measurements of aerosol chemical components in China, as well as aerosol composition network in the United States, MTEA is proved to be able to successfully capture the magnitude and variation of the primary $PM_{2.5}$ (PPM) and secondary $PM_{2.5}$ (SPM). Applying MTEA to China national air quality network, we find that 1) SPM accounts for 63.5% of $PM_{2.5}$ in southern cities of China averaged for 2014-2018, while in the North the proportion drops to 57.1%, and at the same time the secondary proportion in regional background regions is ~19% higher than that in populous regions; 2) the summertime secondary $PM_{2.5}$ proportion presents a slight but consistent increasing trend (from 58.5% to 59.2%) in most populous cities, mainly because of the recent increase in O_3 pollution in China; 3) the secondary $PM_{2.5}$ proportion in Beijing significantly increases by 34% during the COVID-19 lockdown, which might be the main reason of the observed unexpected PM pollution in this special period; and at least, 4) SPM and O_3 show similar positive correlations in the BTH and YRD regions, but the correlations between total $PM_{2.5}$ and O_3 in these two regions are quite different as PPM levels determines. In general, MTEA is a promising tool for efficiently estimating PPM and SPM, and has huge potential for the future PM mitigation.

Keywords: $PM_{2.5}$; Primary and secondary sources; Air quality; O_3; COVID-19

https://doi.org/10.5194/acp-2021-683
Preprint. Discussion started: 5 October 2021


Atmospheric Chemistry and Physics Discussions

1 Introduction

Fine particulate matter ($PM_{2.5}$, aerodynamic diameter less than 2.5 μm) has been the dominant air pollutant in China in the past several years (An et al., 2019; Song et al., 2017; Yang et al., 2016). One source of $PM_{2.5}$ is the direct emission from combustion of fossil/biomass fuel, dust blowing and sea spray, forming primary organic aerosol (POA), elemental carbon (EC), sea salt and mineral dust. The other source is the secondary formation from gaseous precursors emitted by anthropogenic and biogenic activities (Zhu et al., 2018; Wang et al., 2019), generating secondary organic aerosol (SOA) and secondary inorganic aerosol (SIA, sulfate, nitrate and ammonium).

The primary and secondary components of $PM_{2.5}$ have different environmental impacts on air quality, human health and climate change. For example, as a typical primary $PM_{2.5}$ (PPM), EC can severely reduce atmospheric visibility and greatly influence weather and climate due to its strong absorption of solar radiation (Bond et al., 2013; IPCC, 2013; Mao et al., 2017). Sulfate, a critical hygroscopic component of secondary $PM_{2.5}$ (SPM), can be fast formed under high relative humidity condition and further leads to grievous air pollutions (Cheng et al., 2016; Guo et al., 2014; Quan et al., 2015). Furthermore, the sulfate and other hygroscopic $PM_{2.5}$ have considerable influences on climate change mostly by changing cloud properties (Leng et al., 2013; von Schneidemesser et al., 2015). In addition, different $PM_{2.5}$ components also have various deleterious impacts on human health for their toxicities (Hu et al., 2017; Khan et al., 2016; Maji et al., 2018).

Many studies have been conducted on $PM_{2.5}$ components, however, most of them are individual and/or short-term (Guo et al., 2014; Huang et al., 2014b; Ge et al., 2017; Huang et al., 2017; Tao et al., 2017; Ye et al., 2017; Dai et al., 2018; Liu et al., 2018b; Wu et al., 2018; Yu et al., 2019; Zhang et al., 2019). Some studies employed the online aerosol mass spectrometer (AMS) to analyze different $PM_{2.5}$ compositions in Beijing and found that secondary aerosol was the dominant fraction of $PM_{2.5}$ mass concentration during polluted periods (Guo et al., 2014; Quan et al., 2015). Based on offline filter measurements and further laboratory analysis, Liu et al. (2018b) investigated the characteristics of $PM_{2.5}$ components in 12 sites in China (6 urban sites and 6 background sites) for the period of 2012-2013. The result pointed out that the mass concentrations of PPM and SPM and their relative proportions were quite changeable in different regions and seasons. Nevertheless, both the online and offline measurements require a high level of manpower and economic cost, and for this reason, these methods are expensive and rarely applied in large-scale regions or long-

https://doi.org/10.5194/acp-2021-683
Preprint. Discussion started: 5 October 2021


Atmospheric Chemistry and Physics Discussions

term periods.

In this study, we develop a new method, Multi-Tracer Estimation Algorithm (MTEA), with the aim of distinguishing the primary and secondary compositions of $PM_{2.5}$ from routine observation of $PM_{2.5}$ concentration. This algorithm and its application are tested in China and the United States. In section 3, we evaluate the MTEA results comparing with three $PM_{2.5}$ composition data sets, (1) short-term measurements in 16 cities in China from 2012 to 2016 reported by previous studies, (2) continuous long-term measurements in Beijing and Shanghai from 2014 to 2018, and (3) IMPROVE network in the United States during 2014 and 2018. Subsequently, we investigate the spatio-temporal characteristics of PPM and SPM concentrations in China in Section 4.1 and 4.2, explain the unexpected haze event in several cities of China during the COVID-19 lockdown in Section 4.3 and discuss the complicated correlation between PM and O_3 in Section 4.4. This study is different from previous works as follows: (1) we develop an efficient approach to explore PPM and SPM with low economy- and technique-cost, (2) we apply this approach to observation data from the MEE network, offering an unprecedented opportunity to quantify the $PM_{2.5}$ components on a large space and time scale.

2 Methodology

2.1 The Multi-Tracer Estimation Algorithm (MTEA)

In order to distinguish PPM and SPM efficiently from the observed $PM_{2.5}$, we develop a new approach, named Multi-Tracer Estimation Algorithm (MTEA). The multi-tracer (X) is defined to represent multiple primary contributions to $PM_{2.5}$, mainly resulting from incomplete combustion of carbonaceous material and flying dust. We select the typical combustion product CO as one tracer to represent the combustion process, and the particles in coarse mode (PMC, i.e. PM_{10} minus $PM_{2.5}$) as the other tracer to track flying dust. Then, we combine the CO and PMC to generate the multi-tracer X (Eq. 1), which can represent hybrid primary contributions to $PM_{2.5}$.

$$X = a * CO + b * PMC \quad (a + b = 100\%) \quad (1)$$

As shown in Eq. 1, we use a and b to quantify the relative contributions of combustion and dust process to PPM. The values of the coefficients depend on the ratio of emission intensities of POA+EC (combustion products) and fine mode dust, as shown in Eq. 2.

https://doi.org/10.5194/acp-2021-683
Preprint. Discussion started: 5 October 2021

Atmospheric Chemistry and Physics Discussions

$$\frac{a}{b} = \frac{E_{OA} + E_{EC}}{E_{finedust}} = \frac{1.2E_{OC} + E_{EC}}{E_{PM2.5} - (1.2E_{OC} + E_{EC} + E_{SO4} + E_{NO3})} \quad (2)$$

where, E_{OA}, E_{EC}, $E_{finedust}$, E_{OC}, $E_{PM2.5}$, E_{SO4} and E_{NO3} represent the emissions of OA, EC, fine mode dust, OC, $PM_{2.5}$, sulfate and nitrate, respectively. We obtain anthropogenic $PM_{2.5}$, EC and OC emissions in China from Multi-resolution Emission Inventory for China (MEIC, *http://meicmodel.org/*, last access: 1 August 2021) developed by Tsinghua University (Li et al., 2017c). For United States, we retrieve the emission data from the global inventory HTAP (*https://edgar.jrc.ec.europa.eu/htap_v2/index.php?SECURE=123*, last access: 1 August 2021). We further estimate POA emission using POC emission multiply by an empirical factor of 1.2 recommended in literature (Seinfeld and Pandis, 2006), and quantify sulfate and nitrate emissions using $PM_{2.5}$ emission multiply by an investigative coefficient of 0.1 (Zhang 2019). However, the 0.1 might be relatively higher compared to empirical coefficients used in previous simulation studies (0.01-0.05). We evaluated the potential effect of the coefficient, by conducting a set of comparative simulation with the coefficient of 0.03, and found that the final estimated SPM was not sensitive to this coefficient (Table S1). The fine mode dust emission is inferred by the emission of $PM_{2.5}$ deducting the emissions of EC, POA, sulfate and nitrate. Based on Eq. 2, we establish a dynamic "a-b value" database, which can reflect the specific changes of $PM_{2.5}$ sources in terms of different years, seasons, hours and different regions.

With the help of the multi-tracer X, we can descript secondary $PM_{2.5}$ as follows:

$$SPM = PM_{2.5} - PPM \quad (3)$$

$$= PM_{2.5} - \frac{PPM}{X} \times X \quad (4)$$

Here, $PM_{2.5}$ is the observed $PM_{2.5}$ concentration, and the multi-tracer X can be calculated from the observed CO, $PM_{2.5}$ and PM_{10} concentrations. The original concentrations of CO, $PM_{2.5}$ and PM_{10} are normalized for avoiding the influences of their initial levels. To calculate SPM, the key step is to find out the target ratio of PPM/X. In the MTEA method, we give the PPM/X ratio a reasonable range (a range from 0 to 400 is used in this work) and then scan the ratio with an interval of 1. For more precise results, a smaller scanning step can be applied while it may take larger calculation cost. As a result, each varying ratio may obtain a series of SPM, along with a coefficient of determination (R^2) between SPM and X (Fig. S1). If we assume that PPM and SPM came from different sources or processes, then the appropriate PPM/X ratio should be the one that corresponds to weak

https://doi.org/10.5194/acp-2021-683
Preprint. Discussion started: 5 October 2021


Atmospheric Chemistry and Physics Discussions

correlation between SPM and X-tracer. To better understand principle of the MTEA approach, we show the flow chart in Fig. 1. We also provide the MTEA software package and input data sets at *http://nuistairquality.com/m_tea* (last access: 1 August 2021).

The MTEA approach makes some improvement based on the similar principle and assumptions with the modified EC-tracer method developed by Hu et al. (2012). They estimated primary and secondary organic carbon (POC and SOC) concentrations by adopting a proper POC/EC ratio when SOC correlated with EC worst. However, this assumption may be too hard to exist in the real atmosphere. Therefore in the MTEA approach, we take a range of proper ratios of PPM/X when SPM correlates with X-tracer non-significantly (with *p*-value greater than 0.05). As a result, the calculated SPM concentration for each case is a range (Table S2). We employed the concentration ranges to represent the severity of secondary pollution and discussed its uncertainties in the following discussions. While for quantitative calculation, the mean values of the concentration ranges stand for the final estimation.

2.2 $PM_{2.5}$ measurements

2.2.1 $PM_{2.5}$ concentration measurements from the MEE network in China

Focus on the $PM_{2.5}$ pollution in China, MEE set up a comprehensive air quality monitoring network for consistently accessing hourly concentrations of $PM_{2.5}$ as well as SO_2, NO_2, CO, O_3 and PM_{10} since 2013. This network is the most advanced monitoring network currently in China. In this study, we obtained surface observations of hourly $PM_{2.5}$, PM_{10}, CO and O_3 at 334 national monitoring sites in 50 cities from 2014 to 2018 from the MEE public website (*http://106.37.208.233:20035/*, last access: 1 August 2021). 31 among the 50 cities are provincial capital cities, employed to represent populous cities, while the rest 19 relatively small cities are categorized as regional background cities (Table S3). Geographical distribution of those populous and regional background cities is shown in Fig. 2a.

Recently, the Chinese government carried out a series of control policies, such as elimination of backward industry, desulfurization and denitration of flue gas, as well as restriction on motor vehicles (Tang et al., 2019; Wu et al., 2017). Consequently, the concentrations of the major gaseous and particle pollutants have been decreased year by year (Zhai et al., 2019; Shen et al., 2020) . Take $PM_{2.5}$ as an example, previous studies revealed that annual mean $PM_{2.5}$ decreased by 30-50% across China during the period of 2013-2018.

https://doi.org/10.5194/acp-2021-683
Preprint. Discussion started: 5 October 2021


Atmospheric Chemistry and Physics Discussions

2.2.2 $PM_{2.5}$ composition measurements in China

Numerous studies focused on the aerosol chemical composition in China employed offline filter-based observations coupled with laboratory analysis to obtain detailed information of $PM_{2.5}$ compositions. For directly comparing the estimated PPM/SPM with the measured ones in China, we made an evaluation via two long-term time series in-situ measurements in Beijing (Peking University, PKU) and Shanghai (Shanghai Academy of Environment Sciences, SAES) during 2014-2018 (Huang et al., 2019; Tan et al., 2018). The chemical compositions of measurements include ions (NH_4^+, Na^+, K^+ Mg^{2+}, Ca^{2+}, SO_4^{2-}, NO_3^-, Cl^-, by ion chromatography), elements (Al, Si, Ti, Ca, Ti, Mn, etc., through X-ray fluorescence spectrometry), and carbonaceous components (EC and organic carbon, using the thermal-optical transmittance carbon analyzer). After accessing the chemical compositions, we categorized them into PPM and SPM for further evaluation.

In addition, we conducted an investigation about observation-based $PM_{2.5}$ component analyses in 16 cities of China during 2012-2016 from 32 published studies. This survey offered an opportunity for comparing the estimation by MTEA with the past measurements in the terms of the secondary fraction of $PM_{2.5}$.

2.2.3 $PM_{2.5}$ composition measurements from IMPROVE network in the United States

The Interagency Monitoring of Protected Visual Environments (IMPROVE) aerosol network has continuous records of PM_{10}, $PM_{2.5}$ and its chemical speciation in the United States since 1987. The specific aerosol chemical compositions include ammonium sulfate, ammonium nitrate, organic/elemental carbon and soil/mineral dust. More detailed descriptions about IMPORVE are available at *http://vista.cira.colostate.edu/Improve/* (last access: 1 August 2021). Here we extracted the measurements at 104 valid sites in the United States from 2014 to 2018 for the evaluation of MTEA. The spatial distribution of IMPROVE sites used in this work is shown in Fig. 2b. It is noted that IMPROVE program only provides single aerosol component profile every three days. We lowered the time resolution into the monthly average for further evaluation. However, CO is excluded in IMPROVE program. We therefore adopted the Kriging interpolation of CO data based on the hourly archives from the United States EPA (*https://www.epa.gov/outdoor-air-quality-data*, last access: 1 August 2021) as an alternative for model input when running the MTEA.

https://doi.org/10.5194/acp-2021-683
Preprint. Discussion started: 5 October 2021


Atmospheric Chemistry and Physics Discussions

3 Model evaluation

3.1 Evaluation in China

3.1.1 Comparison with continuous long-term measurements in Beijing and Shanghai

We compared the MTEA results with the two sets of long-term in-situ measurements in Beijing and Shanghai, China, and show the evaluations in Fig. 3. Reduced major axis (RMA) regression was applied for fitting the data. In data preprocessing, we removed the in-situ daily measurements whose value was over 30 $\mu g \cdot m^{-3}$ higher than the city average (from MEE).

The comparisons between the estimated and observed PPM in the two cities are given in Fig. 3a and 3c. The correlation coefficient r for predicted PPM versus observed PPM is 0.85 in Beijing and 0.87 in Shanghai. The slope of regression is 1.29 in Beijing and 0.73 in Shanghai, which indicating an overestimation (NMB=32%) or underestimation (NMB=-9%) in these two cities. In terms of SPM, the regression line in Shanghai is quite close to the 1:1 ratio line (s=1.13, d=-2.3), and its statistical correlation is up to 0.89. The estimated SPM in Beijing also shows a high correlation with the observed ones, with its r value exceeds 0.80, though the fitting formula indicates an underestimation of 27%. The discrepancies can be explained by the fact that the observations of primary emission tracers and $PM_{2.5}$ are obtained from different sites. Specifically, the CO and PMC observations are obtained from 12 monitoring MEE sites in Beijing, while the $PM_{2.5}$ component measurements are from single spot at PKU which is away from crowded streets (Tan et al., 2018). The MTEA predictions based on the data from MEE sites located at high-emitting densities district may propose a quite overestimation on PPM concentrations.

Overall, MTEA model performed satisfactorily in case of comparing with the long-term in-situ measurements in Beijing and Shanghai. Nearly all the dots are located at the range between 2:1 ratio and 1:2 ratio. It is believed that our model is able to capture the magnitudes and variations of the PPM and SPM. The comparison about the estimated and the observed inter-annual variations in PPM and SPM would be further discussed in the following texts (sect. 4.2.2).

3.1.2 Comparison with various short-term measurements

To evaluate the reliability of the MTEA approach, we also conducted a literature review for collecting a variety of observation-based $PM_{2.5}$ component analyses in 16 cities of China

https://doi.org/10.5194/acp-2021-683
Preprint. Discussion started: 5 October 2021


Atmospheric Chemistry and Physics Discussions

during 2012-2016 (Chen et al., 2016; Du et al., 2017; Cui et al., 2015; Dai et al., 2018; Gao et al., 2018; Huang et al., 2014a; Huang et al., 2014b; Huang et al., 2017; Jiang et al., 2017; Li et al., 2016; Li et al., 2017a; Lin et al., 2016; Liu et al., 2017; Liu et al., 2014; Liu et al., 2018a; Liu et al., 2018b; Ming et al., 2017; Niu et al., 2016; Tan et al., 2016; Tang et al., 2017; Tao et al., 2017; Tao et al., 2015; Tian et al., 2015; Wang et al., 2018; Wang et al., 2016a; Wang et al., 2016b; Wu et al., 2016; Xu et al., 2019; Yu et al., 2019; Zhang et al., 2015; Zhang et al., 2018; Zhao et al., 2015). Most field measurements focused on regions in eastern China and on episodes during the winter. We listed the concentrations of observed $PM_{2.5}$, SO_4^{2-}, NO_3^-, NH_4^+, and SOA from these studies in Table S4. It should note that there may be inconsistencies in the observation due to different sampling location, observational time and analytical instruments in each study.

The estimated PPM and SPM from MTEA show a reasonable agreement with the observation-based $PM_{2.5}$ component analyses in China. The MTEA estimated secondary proportions of $PM_{2.5}$ (i.e. secondary $PM_{2.5}$ / total $PM_{2.5}$) vary in a range of 41% to 67%, and are higher in eastern cities of China, consistent with the observational results. However, we find that there are still a few discrepancies between the estimated and observation-based results, and the main reasons might be (1) sea salts aerosol contributes a lot to the $PM_{2.5}$ in some coastal cities, but it is unable to be represented by the multi-tracer X, such as the case of Haikou, (2) natural dust plays an important role in $PM_{2.5}$ formation in some western cities, however it cannot be accounted for by anthropogenic emission inventory, such as the case of Lanzhou, and (3) the observation-based results are derived from too few samplers for some cities, such as Lhasa.

3.2 Evaluation in the United States

Based on the chemical component measurements of IMPROVE network, we evaluated the performance of the MTEA model in the United States. Figure 4 presents the scatter plots of the evaluation results, with x-axis indicates the observed concentrations and the y-axis indicates the estimated concentrations. The validation was done in the form of temporal, spatial, as well as spatio-temporal. Each dot represents a monthly mean of either observed or estimated PM concentration.

Almost all of the dots are located at the region between the 2:1 and 1:2 dotted line, indicating that our model is capable of predicting the magnitudes of PPM/SPM in the United

https://doi.org/10.5194/acp-2021-683
Preprint. Discussion started: 5 October 2021


Atmospheric Chemistry and Physics Discussions

States. Based on correlation analysis, we find that the correlation coefficient r for PPM ranges from 0.69 (spatio-temporal validation) to 0.75 (temporal validation), while for SPM, the r is even up to 0.98 (temporal validation). The results reveal that the MTEA approach successfully captured the spatial and temporal variations of PPM and SPM in the United States.

The majority of dots distribute around the 1:1 dotted line. Based on the fitting results, the slopes for regression lines vary from 1.12 (spatial validation) to 1.15 (temporal validation) for PPM and from 0.92 (temporal validation) to 0.93 (spatio-temporal validation) for SPM. In general, PPM and SPM show a slight overestimation and underestimation respectively. The discrepancies may result from the influences of emission inventory. It is reported that the emissions of PMC and CO in the United States continuously declined over the past decade (https://www.statista.com/statistics/501298/volume-of-particulate-matter-2-5-emissions-us/, last access: 2 October 2021). Thus the coefficients a and b derived from HTAP global emission inventory in 2010 overestimate the contribution of primary emissions during the studying period. However, the impacts of emission are inevitable, and we will discuss the uncertainty of emission inventory in Sect. 4.5. In addition, the intercepts of these regression lines for both PPM and SPM are less than ± 0.1 $\mu g \cdot m^{-3}$. The verification results strongly show that our model can reasonably reproduce the monthly averaged concentration of PPM and SPM in the United States.

4 Results and discussion

We used the MTEA approach and the MEE observation data to estimate PPM and SPM concentrations in China for the period of 2014-2018. The observations during severe haze events (top 10% CO and PMC polluted days) were excluded to avoid the influence of extreme high primary emission cases.

4.1 Spatial distribution

Figure 5 shows spatial patterns of the MTEA estimated PPM and SPM concentrations over China averaged for the period of 2014-2018. 16 populous cities and 9 regional background cities in the north, and 15 populous cities and 10 regional background cities in the south (North-South is separated by the Qinling-Huaihe line) are involved in the following discussions.

https://doi.org/10.5194/acp-2021-683
Preprint. Discussion started: 5 October 2021


Atmospheric Chemistry and Physics Discussions

In populous cities, the concentrations of both PPM and SPM in the north (5-year averaged 21.5 $\mu g \cdot m^{-3}$ for PPM and 26.6 $\mu g \cdot m^{-3}$ for SPM) are 15-43% higher than those in the south (15.0 $\mu g \cdot m^{-3}$ for PPM and 23.2 $\mu g \cdot m^{-3}$ for SPM). The North-South difference is mainly caused by the higher energy consumption and consequent stronger pollutant emissions occurring in northern populous regions. Nevertheless, in background regions, the difference is relatively smaller for SPM. The SPM in the South (12.5 $\mu g \cdot m^{-3}$) is only 1% higher than that in the North (12.4 $\mu g \cdot m^{-3}$).

In terms of the secondary proportion of $PM_{2.5}$, the MTEA approach speculates it to be higher in southern regions (63.5%) than that in northern regions (57.1%). The result confirms the fact that atmospheric condition in the South is more favorable for secondary pollutant formation than it is in the North. In addition, the MTEA approach reasonably captures the difference of the secondary proportion of $PM_{2.5}$ between populous and regional background cities. As shown in Fig. 5e and 5f, the secondary proportions of $PM_{2.5}$ in regional background cities are 19% higher than those in populous cities, consistent with recent observational studies (Liu et al., 2018b). Secondary aerosols can affect a larger area than primary aerosols, mostly due to the diffusion of its gaseous precursors. Thus, for regional background regions, the role of secondary $PM_{2.5}$ tends to be more important, mainly caused by the transmitted secondary pollutants from surrounding populous regions.

4.2 Temporal variation

4.2.1 Seasonal variation

We compare seasonal mean concentrations of the MTEA estimated PPM and SPM in 31 populous cities and 19 regional background cities in Table 1. Both the concentrations of PPM and SPM are the highest in winter, with the seasonal mean concentration of 16.6 $\mu g \cdot m^{-3}$ for PPM and 24.9 $\mu g \cdot m^{-3}$ for SPM across China. This phenomenon can be mainly explained by adverse diffusion conditions, such as low boundary layer height and strong temperature inversion (Zhao et al., 2013), as well as fossil-fuel and biofuel usage for winter home heating (Zhang et al., 2009; Zhang and Cao, 2015). Summer is the least polluted season in the year, with the seasonal mean PPM is 10.2 $\mu g \cdot m^{-3}$ and SPM is 15.8 $\mu g \cdot m^{-3}$ nationwide, largely benefiting from the higher boundary layer (Guo et al., 2019) and abundant precipitations.

In terms of the secondary proportion of $PM_{2.5}$, we also compared the secondary contributions in different seasons and in the 50 different Chinese cities (Table 1). The MTEA

https://doi.org/10.5194/acp-2021-683
Preprint. Discussion started: 5 October 2021


Atmospheric Chemistry and Physics Discussions

approach estimates that the secondary proportion tends to be the lowest in fall, with seasonal mean value to be 56.1% nationwide, while for the other three seasons, the seasonal proportions stay around 61%. At the same time, the seasonality of the secondary proportion varies among different regions. In the north of China, the secondary proportions are higher in spring and summer, which is attributed to the stronger atmospheric oxidizing capacity (AOC) in the warmer seasons. But in the south of China, the highest secondary proportions occur in winter, which is mainly explained by the tremendous pollutants (secondary particles and its gaseous precursors) transported from northern China in presence of the monsoon.

4.2.2 Inter-annual variation

Figure 6 illustrates the inter-annual variations of the estimated PPM and SPM based on MTEA in the 31 populous cities and 19 regional background cities of China. We analyzed the MEE observational data during 2014-2018, but excluded the data in 2014 in the regional background regions due to data deficiencies in several cities.

The observed $PM_{2.5}$ concentrations in the populous cities are continuously and significantly reduced since 2014, largely benefiting from a series of emission control measures led by the governments, such as “Action Plan on Prevention and Control of Air Pollution” (Chinese State Council, 2013). Using the MTEA approach, we find that both PPM and SPM are decreased simultaneously, at an annual decreasing rate of 1.9 $\mu g \cdot m^{-3} \cdot yr^{-1}$ and 2.7 $\mu g \cdot m^{-3} \cdot yr^{-1}$, respectively. Consequently, the secondary proportion of $PM_{2.5}$ remains relatively constant (56.4-58.5%). But it presents a consistent increase trend (from 58.5% to 59.2%) in summer during the studying period, which can be attributed to the continuing worsen O_3 pollution. However, for regional background cities, the MTEA approach reports different features of the $PM_{2.5}$ mitigation. The estimated SPM is considerably reduced by 1.1 $\mu g \cdot m^{-3}\ yr^{-1}$ in regional background cities, while the PPM keeps nearly unchanged (decreasing rate is 0.2 $\mu g \cdot m^{-3} \cdot yr^{-1}$). This is because that SPM in regional background cities is largely contributed by pollutants transport from surrounding populous regions, where the air quality is getting better resulting from the aforementioned emission controls. However, the PPM, mostly deriving from local sources, is rarely affected by those emission controls which do mostly focus on densely-populated and industrialized cities but not on background regions.

We discussed the inter-annual variations of PPM and SPM concentration on the basis of long-term in-situ observations in Beijing and Shanghai as well. As Fig. 7 shows, long-term

https://doi.org/10.5194/acp-2021-683
Preprint. Discussion started: 5 October 2021


Atmospheric Chemistry and Physics Discussions

measurements demonstrate a decline of total $PM_{2.5}$ by 4.0 $\mu g \cdot m^{-3}$ yr^{-1} in Beijing (1.6 $\mu g \cdot m^{-3}$ yr^{-1} for PPM and 2.4 $\mu g \cdot m^{-3}$ $yr^{-1}$for SPM) and by 3.9 $\mu g \cdot m^{-3}$ yr^{-1} in Shanghai (1.7 $\mu g \cdot m^{-3}$ yr^{-1} for PM and 2.2 $\mu g \cdot m^{-3}$ $yr^{-1}$for SPM). The observed secondary proportion of $PM_{2.5}$ shows a slight decrease of -0.4% yr^{-1} in Beijing, but a small increase of 0.8% yr^{-1} in Shanghai. Applying the MTEA model to this case, we are delighted to find that our model not only successfully reproduces the consistent decreasing trends of PPM and SPM in Beijing and Shanghai, but also captures the different trends in secondary proportions of $PM_{2.5}$ in the two cities (-0.6% yr^{-1} in Beijing and 0.3% yr^{-1} in Shanghai).

4.3 Application during the COVID-19 lockdown

To curb the spread of the novel Coronavirus Disease 2019 (COVID-19) pandemic, China conducted the entire city's lockdown firstly in Wuhan, Hubei on January 23, 2020. Other provinces gradually implemented this restriction in the following three weeks (Le et al., 2020). The lockdown greatly limited the traffic and outdoor activities, which directly reduced the emissions of primary pollutants (Huang et al., 2020). Through analyzing the MEE monitoring data before (1~23 Jan 2020) and during (24-Jan ~ 17-Feb 2020) the nationwide lockdown (Fig. 8 and Fig. S2), we show that the national mean NO_2, $PM_{2.5}$ and CO concentrations were decreased by 56%, 30% and 24%, respectively, while O_3 posed an increase (34%) in general which would promote the AOC efficiently. However, the surface monitoring network still observed an unexpected $PM_{2.5}$ pollution in cities over BTH region during the lockdown. Especially in Beijing, the mean $PM_{2.5}$ concentration was increased by ~100% compared to its averaged value (41 $\mu g \cdot m^{-3}$) before the nationwide lockdown.

To explore this unexpected air pollution, we find that the enhanced secondary pollution could be the major factor, which even offset the reduction of primary emissions in the BTH region during the lockdown. With the help of MTEA, we tracked variations of the secondary proportions of $PM_{2.5}$ in East China before and during the COVID-19 lockdown (Fig. 8 d-f). The secondary proportions in the BTH region show an evident increase, at the level of 7%-34%, which highlights the importance of the secondary formation during the lockdown. Our result is consistent with recent observation and simulation studies (Chang et al., 2020; Huang et al., 2020; Le et al., 2020), which suggested that the reduced NO_2 resulted in O_3 enhancement, further increasing the AOC and facilitating secondary aerosol formation. In addition, another cause of the air pollution is the unfavorable atmospheric diffusion

https://doi.org/10.5194/acp-2021-683
Preprint. Discussion started: 5 October 2021


Atmospheric Chemistry and Physics Discussions

conditions. CO, a nonreactive pollutant, was increased by 22% in Beijing during the lockdown even under considerable reduction on its emission.

For other regions of China, the MTEA approach suggests the secondary proportions of $PM_{2.5}$ to be increased by 20% over the YRD region, but to be decreased by 32% over the Central China. Although O_3 and AOC had enhanced in all these regions, the unprecedented reductions on precursors ultimately resulted in a net drop of secondary pollution.

4.4 Correlation analysis with O_3

$PM_{2.5}$ and O_3 are closely correlated with each other. One reason is that $PM_{2.5}$ and O_3 have similar precursors, i.e. NO_x and VOCs. Besides, $PM_{2.5}$ can impact O_3 formation through adjusting radiation balance (Li et al., 2018) and affecting radical level via aerosol chemistry (Li et al., 2019). There is therefore a complicated interaction between $PM_{2.5}$ and O_3. Our study utilized MTEA approach for exploring the relationship between PM versus O_3 from the perspective of exploring the statistical correlation.

Figure S3 illustrates the hourly correlations between the estimated SPM versus the observed O_3 averaged for 31 populous cities in China (cities which failed to pass the significant test were excluded) in summer. In general, SPM and O_3 shows a nationwide positive relationship, especially during the afternoon (14:00~18:00, r up to 0.56). This phenomenon might be explained that productions of both O_3 and SPM are simultaneously affected by AOC; thus the higher correlation tend to occur at time of stronger AOC. Moreover, the hourly correlations between SPM and O_3 are higher than that between PPM and O_3 throughout the day, suggesting that secondary oxidation processes may be well captured by the MTEA method.

A series of recent studies have focused on the correlation between $PM_{2.5}$ and O_3, and many of them agreed that the correlation varies greatly in different regions of China, specifically, the correlation is stronger positive in southern cities compared to that in northern cities. Because of this significant difference, a question raises: is the difference mostly caused by PPM, or SPM, or both of them? To address this question, we compare the correlations between daily PPM, SPM and total $PM_{2.5}$ versus O_3 in Beijing-Tianjin-Hebei (BTH) and Yangtze River Delta (YRD) region during the studying period, with the help of META approach. For avoiding the cleaning effects of wet deposition, the days when precipitation took place were removed. Precipitation data is based on the ERA5 reanalysis database from

https://doi.org/10.5194/acp-2021-683
Preprint. Discussion started: 5 October 2021


Atmospheric Chemistry and Physics Discussions

the European Centre for Medium-Range Weather Forecasts (ECMWF, *https://www.ecmwf.int/*, last access, 1 August 2021).

As shown in Fig. 9, the correlations between total $PM_{2.5}$ and O_3 are positive and are stronger in YRD (r=0.14) than in BTH (r=0.09). However, compared with total $PM_{2.5}$, the correlations between SPM and O_3 are much stronger (r=0.21-0.24) and shows minor regional differences, but for PPM, its correlation with O_3 is not significant (p-value>0.05) in both regions. The higher correlation between SPM and O_3 is mostly because that both of them are secondary oxidation products. Higher ambient O_3 concentration indicates stronger AOC, and further lead to more SPM generation. However, for PPM, its effect on O_3 is mainly to inhibit the production of O_3 via adjusting radiation balance and affecting radical level. Hence, we suggest that the regional differences in the correlation between total $PM_{2.5}$ and O_3 are mainly caused by the different PPM levels in BTH and YRD regions.

4.5 Uncertainties

Based on the previous evaluation and discussions, we believe that the MTEA can successfully capture the magnitudes and spatio-temporal variations of PPM and SPM in China. However, these are still some uncertainties in the model estimation and its application in China.

Firstly, the assumption of non-significant correlation between PPM versus SPM may be violated by the fact that SO_2 and NO_x emitted from combustions which will further generate secondary sulfate and nitrate particulates. Nevertheless, the combustion processes for generating SO_2/NO_x and PPM are still different. PPM, i.e. BC and POC, mainly comes from incomplete combustion of residential activities, such as burning biofuels and coal (Long et al., 2013), but SO_2 and NO_x mainly come from the complete combustion process of industrial and transportation sources, such coal, gasoline and diesel (Lu et al., 2011; Li et al., 2017b; Tang et al., 2019). In addition, the MTEA approach uses the assumption of non-significant correlation rather than irrelevance. Such processing also reduces the uncertainty to a certain extent.

Secondly, natural sources of PPM, such as fine dust from desert and sea salt, are not taken into account in the MTEA approach. As a result, PPM in the city near a desert or sea could be underestimated. For example, the $PM_{2.5}$ components observational campaign conducted in 2015 showed that the contribution of sea salt aerosols to ambient $PM_{2.5}$ mass

https://doi.org/10.5194/acp-2021-683
Preprint. Discussion started: 5 October 2021


Atmospheric Chemistry and Physics Discussions

concentration in Haikou is 3.6-8.3% (Liu et al., 2017).

Thirdly, current bottom-up emission inventories are generally outdated with a time lag of at least 1-2 years, mainly due to the lack of timely and accurate statistics. Consequently, the adjoint uncertainty in MTEA estimation is inevitable. To evaluate the uncertainty, a comparison test was conducted by changing the emission coefficient (the *a* and *b* in Eq. 1) with ±10%. The results are presented in Table S5 and point out that the estimated secondary proportions of $PM_{2.5}$ varied less than ±3% in most Chinese cities causing by the changes of the emission coefficient.

5 Conclusions

In this study, we developed a new approach MTEA to distinguish the primary and secondary compositions of $PM_{2.5}$ efficiently from routine observation of $PM_{2.5}$ concentration. By comparing with long-term and short-term measurements of aerosol chemical components in China as well as aerosol composition network in the United States, we showed that MTEA was able to capture variations of PPM and SPM concentrations.

The method was then applied to the surface air pollutant concentrations from MEE observation network in China, and offered an effective way to understand the characteristics of PPM and SPM covering a wide area. In terms of spatial pattern, MTEA reveals that SPM accounts for 63.5% of total $PM_{2.5}$ in southern cities averaged for 2014-2018, while in the North the proportion drops to 57.1%. It should be noted that the secondary proportion in regional background regions is ~19% higher than that in populous regions. In terms of seasonality, the estimated national averaged secondary proportion is the lowest in fall (56.1%), and for the other three seasons it stays among 61%.

Moreover, we applied MTEA to explore the changes of secondary proportion in $PM_{2.5}$ in China. In recent years, the $PM_{2.5}$ pollution in China has been significantly alleviated benefiting from a series of emission control measures. The MTEA results suggest that both PPM and SPM are decreased simultaneously in populous regions, while for regional background regions, the reduction of secondary $PM_{2.5}$ are much more notable than the PPM. The secondary proportion of $PM_{2.5}$ in populous cities during 2014-2018 keeps constant (56.4-58.5%) in general on an annual average scale, but it poses a slight but consistent increase in summer, mostly due to the elevated O_3 and stronger photochemistry pollution in China. In addition, with the help of MTEA, we found that the secondary $PM_{2.5}$ proportion in Beijing

https://doi.org/10.5194/acp-2021-683
Preprint. Discussion started: 5 October 2021


Atmospheric Chemistry and Physics Discussions

significantly increased by 34% during the COVID-19 lockdown, which might be the main reason of the observed unexpected PM pollution in this special period.

Finally, we applied MTEA to explore the synergistic correlation between $PM_{2.5}$ and O_3. Estimated results demonstrate that PPM is weakly correlated with O_3, its effect on O_3 is mainly to inhibit the production of O_3 via adjusting radiation balance and affecting radical level. While SPM is positive correlated with O_3 in presence of the effect of AOC. Higher ambient O_3 concentration indicates stronger AOC, and further lead to more SPM generation. We suggested that the regional differences in the correlation between total $PM_{2.5}$ and O_3 are mainly caused by the different PPM levels in BTH and YRD regions.

China has been plagued by $PM_{2.5}$ pollution in recent years. Different $PM_{2.5}$ compositions may have varying impacts on environment, climate and health, due to the different sources and generation pathways. Therefore, it's of great importance to quantify PPM and SPM for the pollution recognition and prevention. Traditional methods to quantify different $PM_{2.5}$ components are often based on either lab analysis of offline filter samplings or online observation instruments such as AMS. However, these methods are often labor-intensive, strict technical and high economic cost. Our study develops an efficient approach to explore PPM and SPM with low economy- and technique-cost, and applying this approach to large-scale observation networks, such as the MEE network, can offer an unprecedented opportunity to quantify the $PM_{2.5}$ components on a large space and time scale.

Code and Data availability. The MTEA software package and input datasets are available at http://nuistairquality.com/m_tea. Observational datasets and modeling results in the text are available upon request to the corresponding author (linan@nuist.edu.cn).

Author contribution. NL designed this study. NL and HL supervised this work. HRZ and KQT established, performed and improved MTEA model. HRZ and NL interpreted the data and wrote the original draft. CH, HLW, SG and MH provided the long-term measurements of aerosol compositions. HL, CS, JLH, XLG, MDC, ZXL and HY provided useful comments on the paper, and all authors contributed to the revision of the manuscript.

Competing interests. The authors declare that they have no conflict of interest.

https://doi.org/10.5194/acp-2021-683
Preprint. Discussion started: 5 October 2021

Atmospheric Chemistry and Physics Discussions

Acknowledgements. This work was supported by the National Key Research and Development Program of China (2018YFC0213802 and 2019YFA0606804), the National Natural Science Foundation of China (41975171), and the Major Research Plan of the National Social Science Foundation (18ZDA052). The numerical calculations in this paper have been done on the supercomputing system in the Supercomputing Center of Nanjing University of Information Science & Technology.

https://doi.org/10.5194/acp-2021-683
Preprint. Discussion started: 5 October 2021

Atmospheric Chemistry and Physics Discussions

References

Action Plan on Air Pollution Prevention and Control: available at : http://www.mee.gov.cn/gkml/hbb/bwj/201407/t20140725_280516.htm, 2013.

An, Z., Huang, R. J., Zhang, R., Tie, X., Li, G., Cao, J., Zhou, W., Shi, Z., Han, Y., Gu, Z., and Ji, Y.: Severe haze in northern China: A synergy of anthropogenic emissions and atmospheric processes, Proc. Natl. Acad. Sci., 116, 8657-8666, 10.1073/pnas.1900125116, 2019.

Bond, T. C., Doherty, S. J., Fahey, D. W., Forster, P. M., Berntsen, T., DeAngelo, B. J., Flanner, M. G., Ghan, S., Kärcher, B., Koch, D., Kinne, S., Kondo, Y., Quinn, P. K., Sarofim, M. C., Schultz, M. G., Schulz, M., Venkataraman, C., Zhang, H., Zhang, S., Bellouin, N., Guttikunda, S. K., Hopke, P. K., Jacobson, M. Z., Kaiser, J. W., Klimont, Z., Lohmann, U., Schwarz, J. P., Shindell, D., Storelvmo, T., Warren, S. G., and Zender, C. S.: Bounding the role of black carbon in the climate system: A scientific assessment, J. Geophys. Res. , 118, 5380-5552, 10.1002/jgrd.50171, 2013.

Chang, Y., Huang, R. J., Ge, X., Huang, X., Hu, J., Duan, Y., Zou, Z., Liu, X., and Lehmann, M. F.: Puzzling Haze Events in China During the Coronavirus (COVID‐19) Shutdown, Geophys. Res. Lett., 47, 10.1029/2020gl088533, 2020.

Chen, W., Wang, X., Zhou, S., Cohen, J., Zhang, J., Wang, Y., Chang, M., Zeng, Y., Liu, Y., Lin, Z., Liang, G., and Qiu, X.: Chemical Composition of $PM_{2.5}$ and its Impact on Visibility in Guangzhou, Southern China, Aerosol Air Qual. Res., 16, 10.4209/aaqr.2016.02.0059, 2016.

Cheng, Y., Zheng, G., Wei, C., Mu, Q., Zheng, B., Wang, Z., Gao, M., Zhang, Q., He, K., Carmichael, G., Pöschl, U., and Su, H.: Reactive nitrogen chemistry in aerosol water as a source of sulfate during haze events in China, Sci. Adv., 2, e1601530, 10.1126/sciadv.1601530, 2016.

Cui, H., Chen, W., Dai, W., Liu, H., Wang, X., and He, K.: Source apportionment of $PM_{2.5}$ in Guangzhou combining observation data analysis and chemical transport model simulation, Atmos. Environ., 116, 262-271, 10.1016/j.atmosenv.2015.06.054, 2015.

Dai, Q., Bi, X., Liu, B., Li, L., Ding, J., Song, W., Bi, S., Schulze, B. C., Song, C., Wu, J., Zhang, Y., Feng, Y., and Hopke, P. K.: Chemical nature of $PM_{2.5}$ and PM_{10} in Xi'an, China: Insights into primary emissions and secondary particle formation, Environ. Pollut., 240, 155-166, 10.1016/j.envpol.2018.04.111, 2018.

Du, W., Zhang, Y., Chen, Y., Xu, L., Chen, J., Deng, J., Hong, Y., and Xiao, H.: Chemical Characterization and Source Apportionment of $PM_{2.5}$ during Spring and Winter in the Yangtze River Delta, China, Aerosol Air Qual. Res., 17, 2165-2180, 10.4209/aaqr.2017.03.0108, 2017.

Gao, J., Wang, K., Wang, Y., Liu, S., Zhu, C., Hao, J., Liu, H., Hua, S., and Tian, H.: Temporal-spatial characteristics and source apportionment of $PM_{2.5}$ as well as its associated chemical species in the Beijing-Tianjin-Hebei region of China, Environ. Pollut., 233, 714-724, 10.1016/j.envpol.2017.10.123, 2018.

Ge, X., Li, L., Chen, Y., Chen, H., Wu, D., Wang, J., Xie, X., Ge, S., Ye, Z., Xu, J., and Chen, M.: Aerosol characteristics and sources in Yangzhou, China resolved by offline aerosol mass spectrometry and other techniques, Environ. Pollut., 225, 74-85, 10.1016/j.envpol.2017.03.044, 2017.

Guo, J., Li, Y., Cohen, J. B., Li, J., Chen, D., Xu, H., Liu, L., Yin, J., Hu, K., and Zhai, P.:

https://doi.org/10.5194/acp-2021-683
Preprint. Discussion started: 5 October 2021

Shift in the Temporal Trend of Boundary Layer Height in China Using Long-Term (1979–2016) Radiosonde Data, Geophys. Res. Lett., 46, 6080-6089, 10.1029/2019gl082666, 2019.

Guo, S., Hu, M., Zamora, M. L., Peng, J., Shang, D., Zheng, J., Du, Z., Wu, Z., Shao, M., Zeng, L., Molina, M. J., and Zhang, R.: Elucidating severe urban haze formation in China, Proc. Natl. Acad. Sci., 111, 17373-17378, 10.1073/pnas.1419604111, 2014.

Hu, J., Huang, L., Chen, M., Liao, H., Zhang, H., Wang, S., Zhang, Q., and Ying, Q.: Premature Mortality Attributable to Particulate Matter in China: Source Contributions and Responses to Reductions, Environ. Sci. Technol., 51, 9950-9959, 10.1021/acs.est.7b03193, 2017.

Hu, W. W., Hu, M., Deng, Z. Q., Xiao, R., Kondo, Y., Takegawa, N., Zhao, Y. J., Guo, S., and Zhang, Y. H.: The characteristics and origins of carbonaceous aerosol at a rural site of PRD in summer of 2006, Atmos. Chem. Phys., 12, 1811-1822, 10.5194/acp-12-1811-2012, 2012.

Huang, G., Cheng, T., Zhang, R., Tao, J., Leng, C., Zhang, Y., Zha, S., Zhang, D., Li, X., and Xu, C.: Optical properties and chemical composition of $PM_{2.5}$ in Shanghai in the spring of 2012, Particuology, 13, 52-59, 10.1016/j.partic.2013.10.005, 2014a.

Huang, L., An, J., Koo, B., Yarwood, G., Yan, R., Wang, Y., Huang, C., and Li, L.: Sulfate formation during heavy winter haze events and the potential contribution from heterogeneous SO₂ + NO₂ reactions in the Yangtze River Delta region, China, Atmospheric Chemistry and Physics, 19, 14311-14328, 10.5194/acp-19-14311-2019, 2019.

Huang, R. J., Zhang, Y., Bozzetti, C., Ho, K. F., Cao, J. J., Han, Y., Daellenbach, K. R., Slowik, J. G., Platt, S. M., Canonaco, F., Zotter, P., Wolf, R., Pieber, S. M., Bruns, E. A., Crippa, M., Ciarelli, G., Piazzalunga, A., Schwikowski, M., Abbaszade, G., Schnelle-Kreis, J., Zimmermann, R., An, Z., Szidat, S., Baltensperger, U., El Haddad, I., and Prevot, A. S.: High secondary aerosol contribution to particulate pollution during haze events in China, Nature, 514, 218-222, 10.1038/nature13774, 2014b.

Huang, X., Liu, Z., Liu, J., Hu, B., Wen, T., Tang, G., Zhang, J., Wu, F., Ji, D., Wang, L., and Wang, Y.: Chemical characterization and source identification of $PM_{2.5}$ at multiple sites in the Beijing–Tianjin–Hebei region, China, Atmos. Chem. Phys., 17, 12941-12962, 10.5194/acp-17-12941-2017, 2017.

Huang, X., Ding, A., Gao, J., Zheng, B., Zhou, D., Qi, X., Tang, R., Wang, J., Ren, C., Nie, W., Chi, X., Xu, Z., Chen, L., Li, Y., Che, F., Pang, N., Wang, H., Tong, D., Qin, W., Cheng, W., Liu, W., Fu, Q., Liu, B., Chai, F., Davis, S. J., Zhang, Q., and He, K.: Enhanced secondary pollution offset reduction of primary emissions during COVID-19 lockdown in China, Nat. Sci. Rev., 10.1093/nsr/nwaa137, 2020.

IPCC: Climate Change 2013: The Physical Science Basis, Cambridge University Press, United Kingdom and New York, NY, USA, 2013.

Jiang, N., Guo, Y., Wang, Q., Kang, P., Zhang, R., and Tang, X.: Chemical Composition Characteristics of $PM_{2.5}$ in Three Cities in Henan, Central China, Aerosol Air Qual. Res., 17, 2367-2380, 10.4209/aaqr.2016.10.0463, 2017.

Khan, M. F., Latif, M. T., Saw, W. H., Amil, N., Nadzir, M. S. M., Sahani, M., Tahir, N. M., and Chung, J. X.: Fine particulate matter in the tropical environment: monsoonal effects, source apportionment, and health risk assessment, Atmos. Chem. Phys., 16, 597-617,

https://doi.org/10.5194/acp-2021-683
Preprint. Discussion started: 5 October 2021

10.5194/acp-16-597-2016, 2016.

Le, T., Wang, Y., Liu, L., Yang, J., Yung, Y. L., Li, G., and Seinfeld, J. H.: Unexpected air pollution with marked emission reductions during the COVID-19 outbreak in China, Science, eabb7431, 10.1126/science.abb7431, 2020.

Leng, C., Cheng, T., Chen, J., Zhang, R., Tao, J., Huang, G., Zha, S., Zhang, M., Fang, W., Li, X., and Li, L.: Measurements of surface cloud condensation nuclei and aerosol activity in downtown Shanghai, Atmos. Environ., 69, 354-361, 10.1016/j.atmosenv.2012.12.021, 2013.

Li, H., Wang, Q. g., Yang, M., Li, F., Wang, J., Sun, Y., Wang, C., Wu, H., and Qian, X.: Chemical characterization and source apportionment of $PM_{2.5}$ aerosols in a megacity of Southeast China, Atmos. Res., 181, 288-299, 10.1016/j.atmosres.2016.07.005, 2016.

Li, K., Jacob, D. J., Liao, H., Shen, L., Zhang, Q., and Bates, K. H.: Anthropogenic drivers of 2013-2017 trends in summer surface ozone in China, Proc. Natl. Acad. Sci., 116, 422-427, 10.1073/pnas.1812168116, 2019.

Li, L., Tan, Q., Zhang, Y., Feng, M., Qu, Y., An, J., and Liu, X.: Characteristics and source apportionment of $PM_{2.5}$ during persistent extreme haze events in Chengdu, southwest China, Environ. Pollut., 230, 718-729, 10.1016/j.envpol.2017.07.029, 2017a.

Li, M., Liu, H., Geng, G., Hong, C., Liu, F., Song, Y., Tong, D., Zheng, B., Cui, H., Man, H., Zhang, Q., and He, K.: Anthropogenic emission inventories in China: a review, Natl. Sci. Rev., 4, 834-866, 10.1093/nsr/nwx150, 2017b.

Li, M., Zhang, Q., Kurokawa, J. I., Woo, J. H., He, K., Lu, Z., Ohara, T., Song, Y., Streets, D. G., Carmichael, G. R., Cheng, Y., Hong, C., Huo, H., Jiang, X., Kang, S., Liu, F., Su, H., and Zheng, B.: MIX: a mosaic Asian anthropogenic emission inventory under the international collaboration framework of the MICS-Asia and HTAP, Atmos. Chem. Phys., 17, 935-963, 10.5194/acp-17-935-2017, 2017c.

Li, N., He, Q., Greenberg, J., Guenther, A., Li, J., Cao, J., Wang, J., Liao, H., Wang, Q., and Zhang, Q.: Impacts of biogenic and anthropogenic emissions on summertime ozone formation in the Guanzhong Basin, China, Atmos. Chem. Phys., 18, 7489-7507, 10.5194/acp-18-7489-2018, 2018.

Lin, Y. C., Hsu, S. C., Chou, C. C., Zhang, R., Wu, Y., Kao, S. J., Luo, L., Huang, C. H., Lin, S. H., and Huang, Y. T.: Wintertime haze deterioration in Beijing by industrial pollution deduced from trace metal fingerprints and enhanced health risk by heavy metals, Environ. Pollut., 208, 284-293, 10.1016/j.envpol.2015.07.044, 2016.

Liu, B., Li, T., Yang, J., Wu, J., Wang, J., Gao, J., Bi, X., Feng, Y., Zhang, Y., and Yang, H.: Source apportionment and a novel approach of estimating regional contributions to ambient $PM_{2.5}$ in Haikou, China, Environ. Pollut., 223, 334-345, 10.1016/j.envpol.2017.01.030, 2017.

Liu, J., Li, J., Zhang, Y., Liu, D., Ding, P., Shen, C., Shen, K., He, Q., Ding, X., Wang, X., Chen, D., Szidat, S., and Zhang, G.: Source apportionment using radiocarbon and organic tracers for $PM_{2.5}$ carbonaceous aerosols in Guangzhou, South China: contrasting local- and regional-scale haze events, Environ. Sci. Technol., 48, 12002-12011, 10.1021/es503102w, 2014.

Liu, W., Xu, Y., Liu, W., Liu, Q., Yu, S., Liu, Y., Wang, X., and Tao, S.: Oxidative potential of ambient $PM_{2.5}$ in the coastal cities of the Bohai Sea, northern China: Seasonal variation and source apportionment, Environ. Pollut., 236, 514-528, 10.1016/j.envpol.2018.01.116,

https://doi.org/10.5194/acp-2021-683
Preprint. Discussion started: 5 October 2021

2018a.

Liu, Z., Gao, W., Yu, Y., Hu, B., Xin, J., Sun, Y., Wang, L., Wang, G., Bi, X., Zhang, G., Xu, H., Cong, Z., He, J., Xu, J., and Wang, Y.: Characteristics of $PM_{2.5}$ mass concentrations and chemical species in urban and background areas of China: emerging results from the CARE-China network, Atmos. Chem. Phys., 18, 8849-8871, 10.5194/acp-18-8849-2018, 2018b.

Long, C. M., Nascarella, M. A., and Valberg, P. A.: Carbon black vs. black carbon and other airborne materials containing elemental carbon: physical and chemical distinctions, Environ. Pollut., 181, 271-286, 10.1016/j.envpol.2013.06.009, 2013.

Lu, Z., Zhang, Q., and Streets, D. G.: Sulfur dioxide and primary carbonaceous aerosol emissions in China and India, 1996–2010, Atmos. Chem. Phys., 11, 9839-9864, 10.5194/acp-11-9839-2011, 2011.

Maji, K. J., Ye, W. F., Arora, M., and Shiva Nagendra, S. M.: $PM_{2.5}$-related health and economic loss assessment for 338 Chinese cities, Environ. Int., 121, 392-403, 10.1016/j.envint.2018.09.024, 2018.

Mao, Y.-H., Liao, H., and Chen, H.-S.: Impacts of East Asian summer and winter monsoons on interannual variations of mass concentrations and direct radiative forcing of black carbon over eastern China, Atmos. Chem. Phys., 17, 4799-4816, 10.5194/acp-17-4799-2017, 2017.

Ming, L., Jin, L., Li, J., Fu, P., Yang, W., Liu, D., Zhang, G., Wang, Z., and Li, X.: $PM_{2.5}$ in the Yangtze River Delta, China: Chemical compositions, seasonal variations, and regional pollution events, Environ. Pollut., 223, 200-212, 10.1016/j.envpol.2017.01.013, 2017.

Niu, X., Cao, J., Shen, Z., Ho, S. S. H., Tie, X., Zhao, S., Xu, H., Zhang, T., and Huang, R.: $PM_{2.5}$ from the Guanzhong Plain: Chemical composition and implications for emission reductions, Atmos. Environ., 147, 458-469, 10.1016/j.atmosenv.2016.10.029, 2016.

Quan, J., Liu, Q., Li, X., Gao, Y., Jia, X., Sheng, J., and Liu, Y.: Effect of heterogeneous aqueous reactions on the secondary formation of inorganic aerosols during haze events, Atmos. Environ., 122, 306-312, 10.1016/j.atmosenv.2015.09.068, 2015.

Seinfeld, J. H., and Pandis, S. N.: Atmospheric chemistry and physics: From air pollution to climate change, Third edition, John Wiley, New York, 2006.

Shen, F., Zhang, L., Jiang, L., Tang, M., Gai, X., Chen, M., and Ge, X.: Temporal variations of six ambient criteria air pollutants from 2015 to 2018, their spatial distributions, health risks and relationships with socioeconomic factors during 2018 in China, Environ. Int., 137, 10.1016/j.envint.2020.105556, 2020.

Song, C., Wu, L., Xie, Y., He, J., Chen, X., Wang, T., Lin, Y., Jin, T., Wang, A., Liu, Y., Dai, Q., Liu, B., Wang, Y. N., and Mao, H.: Air pollution in China: Status and spatiotemporal variations, Environ. Pollut., 227, 334-347, 10.1016/j.envpol.2017.04.075, 2017.

Tan, J., Xiang, P., Zhou, X., Duan, J., Ma, Y., He, K., Cheng, Y., Yu, J., and Querol, X.: Chemical characterization of humic-like substances (HULIS) in $PM_{2.5}$ in Lanzhou, China, Sci. Total Environ., 573, 1481-1490, 10.1016/j.scitotenv.2016.08.025, 2016.

Tan, T., Hu, M., Li, M., Guo, Q., Wu, Y., Fang, X., Gu, F., Wang, Y., and Wu, Z.: New insight into PM2.5 pollution patterns in Beijing based on one-year measurement of chemical compositions, Sci. Total Environ., 621, 734-743, 10.1016/j.scitotenv.2017.11.208, 2018.

https://doi.org/10.5194/acp-2021-683
Preprint. Discussion started: 5 October 2021

Tang, L., Qu, J., Mi, Z., Bo, X., Chang, X., Anadon, L. D., Wang, S., Xue, X., Li, S., Wang, X., and Zhao, X.: Substantial emission reductions from Chinese power plants after the introduction of ultra-low emissions standards, Nat. Energy, 4, 929-938, 10.1038/s41560-019-0468-1, 2019.

Tang, X., Chen, X., and Tian, Y.: Chemical composition and source apportionment of $PM_{2.5}$ – A case study from one year continuous sampling in the Chang-Zhu-Tan urban agglomeration, Atmos. Pollut. Res., 8, 885-899, 10.1016/j.apr.2017.02.004, 2017.

Tao, J., Zhang, L., Gao, J., Wang, H., Chai, F., and Wang, S.: Aerosol chemical composition and light scattering during a winter season in Beijing, Atmos. Environ., 110, 36-44, 10.1016/j.atmosenv.2015.03.037, 2015.

Tao, J., Zhang, L., Cao, J., Zhong, L., Chen, D., Yang, Y., Chen, D., Chen, L., Zhang, Z., Wu, Y., Xia, Y., Ye, S., and Zhang, R.: Source apportionment of $PM_{2.5}$ at urban and suburban areas of the Pearl River Delta region, south China - With emphasis on ship emissions, Sci. Total Environ., 574, 1559-1570, 10.1016/j.scitotenv.2016.08.175, 2017.

Tian, P., Wang, G., Zhang, R., Wu, Y., and Yan, P.: Impacts of aerosol chemical compositions on optical properties in urban Beijing, China, Particuology, 18, 155-164, 10.1016/j.partic.2014.03.014, 2015.

von Schneidemesser, E., Monks, P. S., Allan, J. D., Bruhwiler, L., Forster, P., Fowler, D., Lauer, A., Morgan, W. T., Paasonen, P., Righi, M., Sindelarova, K., and Sutton, M. A.: Chemistry and the Linkages between Air Quality and Climate Change, Chem. Rev., 115, 3856-3897, 10.1021/acs.chemrev.5b00089, 2015.

Wang, H., Tian, M., Chen, Y., Shi, G., Liu, Y., Yang, F., Zhang, L., Deng, L., Yu, J., Peng, C., and Cao, X.: Seasonal characteristics, formation mechanisms and source origins of $PM_{2.5}$ in two megacities in Sichuan Basin, China, Atmos. Chem. Phys., 18, 865-881, 10.5194/acp-18-865-2018, 2018.

Wang, H. L., Qiao, L. P., Lou, S. R., Zhou, M., Ding, A. J., Huang, H. Y., Chen, J. M., Wang, Q., Tao, S. K., Chen, C. H., Li, L., and Huang, C.: Chemical composition of $PM_{2.5}$ and meteorological impact among three years in urban Shanghai, China, J. of Clean. Prod., 112, 1302-1311, 10.1016/j.jclepro.2015.04.099, 2016a.

Wang, Y., Jia, C., Tao, J., Zhang, L., Liang, X., Ma, J., Gao, H., Huang, T., and Zhang, K.: Chemical characterization and source apportionment of $PM_{2.5}$ in a semi-arid and petrochemical-industrialized city, Northwest China, Sci. Total Environ., 573, 1031-1040, 10.1016/j.scitotenv.2016.08.179, 2016b.

Wang, Y., Chen, J., Wang, Q., Qin, Q., Ye, J., Han, Y., Li, L., Zhen, W., Zhi, Q., Zhang, Y., and Cao, J.: Increased secondary aerosol contribution and possible processing on polluted winter days in China, Environ. Int., 127, 78-84, 10.1016/j.envint.2019.03.021, 2019.

Wu, J., Xu, C., Wang, Q., and Cheng, W.: Potential Sources and Formations of the $PM_{2.5}$ Pollution in Urban Hangzhou, Atmosphere, 7, 100, 10.3390/atmos7080100, 2016.

Wu, X., Vu, T. V., Shi, Z., Harrison, R. M., Liu, D., and Cen, K.: Characterization and source apportionment of carbonaceous $PM_{2.5}$ particles in China - A review, Atmos. Environ., 189, 187-212, 10.1016/j.atmosenv.2018.06.025, 2018.

Wu, Y., Zhang, S., Hao, J., Liu, H., Wu, X., Hu, J., Walsh, M. P., Wallington, T. J., Zhang, K. M., and Stevanovic, S.: On-road vehicle emissions and their control in China: A review and outlook, Sci. Total Environ., 574, 332-349, 10.1016/j.scitotenv.2016.09.040, 2017.

https://doi.org/10.5194/acp-2021-683
Preprint. Discussion started: 5 October 2021

Xu, H., Xiao, Z., Chen, K., Tang, M., Zheng, N., Li, P., Yang, N., Yang, W., and Deng, X.: Spatial and temporal distribution, chemical characteristics, and sources of ambient particulate matter in the Beijing-Tianjin-Hebei region, Sci. Total Environ., 658, 280-293, 10.1016/j.scitotenv.2018.12.164, 2019.

Yang, Y., Liao, H., and Lou, S.: Increase in winter haze over eastern China in recent decades: Roles of variations in meteorological parameters and anthropogenic emissions, J. Geophys. Res., 121, 13,050-013,065, 10.1002/2016jd025136, 2016.

Ye, Z., Liu, J., Gu, A., Feng, F., Liu, Y., Bi, C., Xu, J., Li, L., Chen, H., Chen, Y., Dai, L., Zhou, Q., and Ge, X.: Chemical characterization of fine particulate matter in Changzhou, China, and source apportionment with offline aerosol mass spectrometry, Atmos. Chem. Phys., 17, 2573-2592, 10.5194/acp-17-2573-2017, 2017.

Yu, S., Liu, W., Xu, Y., Yi, K., Zhou, M., Tao, S., and Liu, W.: Characteristics and oxidative potential of atmospheric $PM_{2.5}$ in Beijing: Source apportionment and seasonal variation, Sci. Total Environ., 650, 277-287, 10.1016/j.scitotenv.2018.09.021, 2019.

Zhai, S., Jacob, D. J., Wang, X., Shen, L., Li, K., Zhang, Y., Gui, K., Zhao, T., and Liao, H.: Fine particulate matter ($PM_{2.5}$) trends in China, 2013–2018: separating contributions from anthropogenic emissions and meteorology, Atmos. Chem. Phys., 19, 11031-11041, 10.5194/acp-19-11031-2019, 2019.

Zhang, H., Cheng, S., Li, J., Yao, S., and Wang, X.: Investigating the aerosol mass and chemical components characteristics and feedback effects on the meteorological factors in the Beijing-Tianjin-Hebei region, China, Environ. Pollut., 244, 495-502, 10.1016/j.envpol.2018.10.087, 2019.

Zhang, Q., G. Streets, D., Carmichael, G., B. He, K., Huo, H., Kannari, A., Klimont, Z., S. Park, I., Reddy, E. S., Fu, J., Chen, D., Duan, L., Lei, Y., Wang, L., and L. Yao, Z.: Asian emissions in 2006 for the NASA INTEX-B mission, Atmos. Chem. Phys., 9, 5131-5153, 10.5194/acpd-9-5131-2009, 2009.

Zhang, Q., Shen, Z., Cao, J., Zhang, R., Zhang, L., Huang, R. J., Zheng, C., Wang, L., Liu, S., Xu, H., Zheng, C., and Liu, P.: Variations in $PM_{2.5}$, TSP, BC, and trace gases (NO_2, SO_2, and O_3) between haze and non-haze episodes in winter over Xi'an, China, Atmos. Environ., 112, 64-71, 10.1016/j.atmosenv.2015.04.033, 2015.

Zhang , Q.: R & D and Application Demonstration of Dynamic Grid Emission Source Information Platform (in Chinese), The Fourth Technical Seminar on Emission Inventory of Air Pollution Sources in China, Nanjing, China, 18-19 September 2019, 2019.

Zhang, Y., Lang, J., Cheng, S., Li, S., Zhou, Y., Chen, D., Zhang, H., and Wang, H.: Chemical composition and sources of PM_1 and $PM_{2.5}$ in Beijing in autumn, Sci. Total Environ., 630, 72-82, 10.1016/j.scitotenv.2018.02.151, 2018.

Zhang, Y. L., and Cao, F.: Fine particulate matter ($PM_{2.5}$) in China at a city level, Sci. Rep., 5, 14884, 10.1038/srep14884, 2015.

Zhao, M., Huang, Z., Qiao, T., Zhang, Y., Xiu, G., and Yu, J.: Chemical characterization, the transport pathways and potential sources of $PM_{2.5}$ in Shanghai: Seasonal variations, Atmos. Res., 158-159, 66-78, 10.1016/j.atmosres.2015.02.003, 2015.

Zhao, X. J., Zhao, P. S., Xu, J., Meng, W., Pu, W. W., Dong, F., He, D., and Shi, Q. F.: Analysis of a winter regional haze event and its formation mechanism in the North China Plain, Atmos. Chem. Phys., 13, 5685-5696, 10.5194/acp-13-5685-2013, 2013.

https://doi.org/10.5194/acp-2021-683
Preprint. Discussion started: 5 October 2021

Atmospheric Chemistry and Physics Discussions

Zhu, Y., Huang, L., Li, J., Ying, Q., Zhang, H., Liu, X., Liao, H., Li, N., Liu, Z., Mao, Y., Fang, H., and Hu, J.: Sources of particulate matter in China: Insights from source apportionment studies published in 1987-2017, Environ. Int., 115, 343-357, 10.1016/j.envint.2018.03.037, 2018.

5

https://doi.org/10.5194/acp-2021-683
Preprint. Discussion started: 5 October 2021

Atmospheric Chemistry and Physics Discussions

Table 1. Seasonal mean concentrations of the primary and secondary $PM_{2.5}$ in 31 populous cities and 19 regional background cities of China.

City	PPM (μg·m^{-3})				SPM (μg·m^{-3})				SPM/$PM_{2.5}$ (%)			
	MAM	JJA	SON	DJF	MAM	JJA	SON	DJF	MAM	JJA	SON	DJF
Populous cities in the Northern China												
Beijing	31.0	28.4	30.6	34.1	25.0	23.7	20.1	16.2	44.7	45.4	39.6	32.2
Tianjin	17.8	13.7	21.9	28.2	42.0	35.3	32.9	29.0	70.2	72.1	60.0	50.7
Shijiazhuang	35.0	22.4	41.5	54.0	36.7	35.5	32.1	37.7	51.2	61.3	43.6	41.1
Taiyuan	22.0	20.2	32.7	32.3	28.4	22.2	21.0	25.0	56.3	52.3	39.1	43.6
Hohhot	13.1	11.4	18.2	20.1	19.2	13.1	16.0	20.7	59.5	53.6	46.8	50.7
Shenyang	21.0	16.7	24.4	27.8	26.1	17.4	20.8	28.0	55.3	51.0	46.0	50.2
Changchun	21.3	15.8	20.2	28.9	18.3	12.3	17.2	25.0	46.2	43.9	46.0	46.4
Harbin	14.1	9.3	15.5	27.2	25.5	15.2	20.9	38.9	64.4	61.9	57.3	58.9
Jinan	25.6	23.0	29.9	32.4	38.2	30.7	30.7	38.3	59.9	57.1	50.7	54.2
Zhengzhou	24.8	20.2	28.6	34.1	45.2	28.8	33.9	44.1	64.6	58.7	54.3	56.4
Lhasa	6.6	5.9	8.2	5.8	13.0	9.2	9.3	13.6	66.3	61.2	53.2	70.1
Xian	24.1	15.3	31.3	37.1	31.5	20.1	24.5	41.3	56.7	56.7	44.0	52.7
Lanzhou	14.1	10.1	17.8	21.3	29.3	24.1	24.8	33.2	67.6	70.4	58.2	60.9
Xining	14.8	12.4	18.3	17.9	26.4	19.3	21.0	34.5	64.1	60.8	53.4	65.9
Yinchuan	12.9	8.2	16.1	18.7	22.8	21.8	21.1	27.0	63.8	72.8	56.7	59.1
Urumqi	15.2	9.5	16.5	27.9	30.9	19.1	32.0	63.6	67.1	66.9	66.0	69.5
Average	19.6	15.2	23.2	28.0	28.7	21.7	23.6	32.3	59.4	58.9	50.4	53.5
Regional background cities in the Northern China												
Weihai	8.1	7.1	8.6	10.7	23.8	18.5	14.9	13.7	74.6	72.2	63.4	56.0
Jiayuguan	7.8	7.0	7.5	7.0	16.6	11.4	14.5	19.2	68.1	61.9	65.9	73.4
Zhangjiakou	10.8	11.0	10.7	10.7	14.2	14.4	12.8	14.4	56.8	56.6	54.5	57.4
Daxinganling	4.3	3.6	4.6	5.7	9.2	7.7	9.3	11.6	68.0	67.9	67.0	66.9
Xilingol	2.3	2.3	2.8	3.1	10.2	9.3	7.7	9.1	81.8	80.1	73.1	74.7
Yanbian	9.9	5.6	9.4	11.7	15.3	9.1	13.5	17.4	60.7	62.1	58.9	59.7
Guyuan	12.3	9.0	11.9	13.1	19.0	13.1	14.7	20.1	60.7	59.2	55.4	60.6
Yushu	4.3	2.1	4.2	3.9	10.0	9.6	7.1	9.9	69.8	82.3	62.7	71.5
Altay	2.0	1.3	1.7	2.7	6.3	6.3	6.0	8.0	76.1	83.5	77.5	74.7
Average	6.9	5.5	6.8	7.6	13.8	11.1	11.2	13.7	66.9	67.0	62.1	64.2
Populous cities in the Southern China												
Shanghai	12.4	11.1	11.7	15.8	29.5	22.5	20.8	25.4	70.4	67.0	64.1	61.6
Nanjing	19.1	16.0	19.9	24.3	29.2	18.7	19.9	28.5	60.4	53.9	50.1	54.0
Hangzhou	21.1	17.8	21.5	23.6	24.9	14.5	18.9	28.5	54.1	45.0	46.8	54.7
Hefei	16.4	14.6	17.9	23.2	39.8	26.7	30.1	39.8	70.9	64.6	62.7	63.2
Fuzhou	9.0	7.5	7.5	7.6	18.0	12.9	13.7	19.7	66.6	63.3	64.7	72.2
Nanchang	14.8	9.8	13.2	15.8	20.6	13.6	22.3	28.8	58.2	58.1	62.9	64.6
Wuhan	18.5	15.6	18.9	25.3	36.4	19.9	30.0	45.3	66.3	56.1	61.3	64.2
Changsha	17.6	13.2	17.5	21.9	31.5	21.1	31.2	40.0	64.1	61.5	64.1	64.6
Guangzhou	11.6	9.5	12.1	12.7	22.6	16.3	23.4	26.6	66.0	63.3	65.9	67.7
Nanning	11.7	9.7	14.9	13.3	22.0	12.9	19.9	28.7	65.3	57.1	57.1	68.3
Haikou	5.8	4.7	8.1	6.0	11.5	6.9	8.7	15.8	66.3	59.4	51.8	72.6
Chongqing	17.9	14.0	18.6	21.6	24.1	19.4	25.0	38.8	57.5	58.0	57.3	64.2
Chengdu	29.6	20.0	27.1	31.7	23.6	15.0	18.2	39.1	44.3	42.8	40.1	55.2
Guiyang	13.5	10.6	12.2	9.9	21.3	12.2	18.5	29.8	61.2	53.6	60.4	75.0
Kunming	9.3	6.5	6.9	8.1	21.1	13.5	16.1	18.4	69.5	67.6	69.9	69.3

https://doi.org/10.5194/acp-2021-683
Preprint. Discussion started: 5 October 2021

Atmospheric Chemistry and Physics Discussions

Average	15.2	12.0	15.2	17.4	25.1	16.4	21.1	30.2	62.2	57.7	58.1	63.5
Regional background cities in the Southern China												
Huangshan	5.3	5.1	5.7	6.4	20.7	11.2	16.3	22.7	79.5	68.8	74.2	78.1
Nanping	6.1	5.0	6.4	5.7	15.9	11.4	13.4	17.4	72.2	69.7	67.9	75.4
Zhoushan	9.5	8.0	8.4	11.9	13.7	10.2	10.1	11.5	59.2	56.2	54.5	49.1
Shanwei	7.9	4.8	8.2	5.7	16.6	10.3	17.4	22.7	67.8	68.2	68.1	79.9
Beihai	7.5	4.2	10.6	8.7	16.4	8.2	16.4	25.8	68.7	65.9	60.6	74.7
Qianxinan	3.3	1.7	2.2	2.9	12.5	12.1	12.2	13.8	79.2	87.9	84.8	82.9
Sanya	4.6	4.2	5.5	3.7	9.7	5.6	6.8	11.7	67.8	56.8	55.4	75.8
Aba	2.0	2.1	2.1	2.9	10.5	10.3	10.3	10.8	84.2	83.0	83.2	78.7
Linzhi	2.3	1.5	2.0	2.1	7.5	6.2	5.3	7.6	76.6	80.5	73.0	78.5
Diqing	1.9	1.5	1.7	1.6	10.5	9.4	9.4	10.2	84.7	86.4	84.8	86.2
Average	5.0	3.8	5.3	5.2	13.4	9.5	11.7	15.4	72.7	71.4	69.1	74.9

https://doi.org/10.5194/acp-2021-683
Preprint. Discussion started: 5 October 2021

Atmospheric Chemistry and Physics Discussions

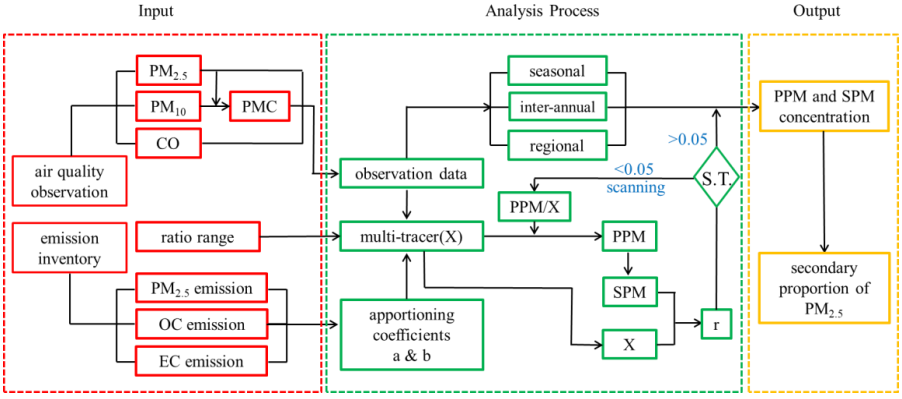

Figure 1. The flow chart of the M-TEA approach. The part in red indicates the air quality data and emission input. The part in green stands for the key process for predicting PPM/SPM based on the routine $PM_{2.5}$ observation. In this part, S.T. means the significant test. The significant level α is set to 0.05. The part in orange indicates the final output.

https://doi.org/10.5194/acp-2021-683
Preprint. Discussion started: 5 October 2021

Atmospheric Chemistry and Physics Discussions

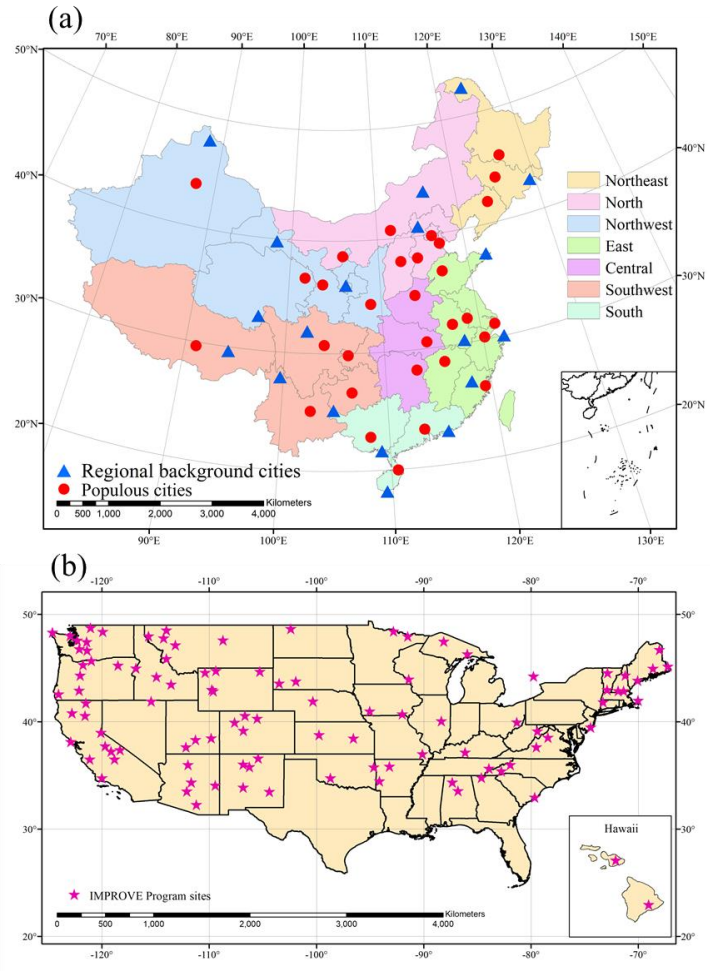

Figure 2. The geographical locations for the observational data used in this study. (a) Geographical locations of 31 populous cities (red circles) and 19 regional background cities (blue triangles) of China in this study. (b) Spatial distribution of the IMPROVE aerosol monitoring network (pink pentagrams) in the United States.

https://doi.org/10.5194/acp-2021-683
Preprint. Discussion started: 5 October 2021

Atmospheric Chemistry and Physics Discussions

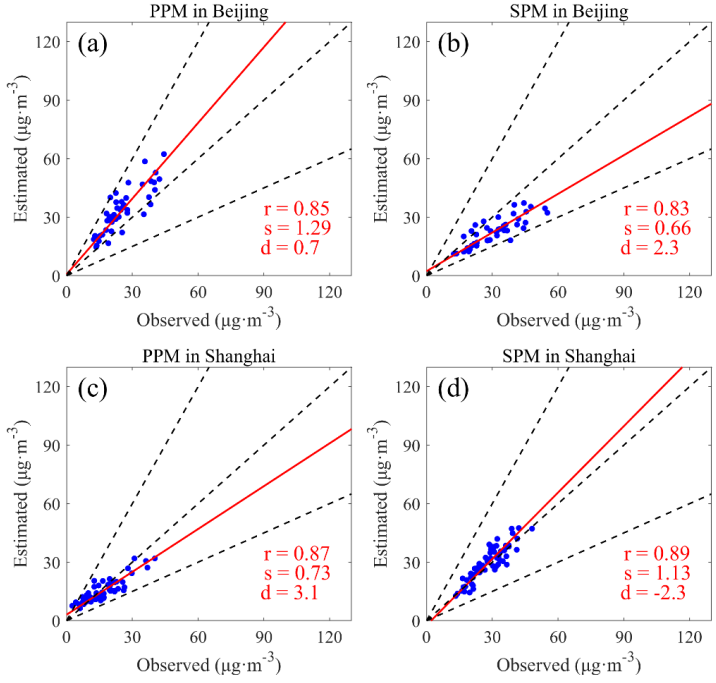

Figure 3. The scatter evaluation between the monthly mean of observed PM versus that of estimated PM in Beijing (a-b) and Shanghai (c-d), China. Panel (a, d), (b, e) denotes PPM and SPM. The red numbers in each panel indicate the Pearson correlation coefficient (r), the slope (s) and the intercept of fitting line (d). The fitting lines in red were based on the Reduced Major Axis (RMA) regression. The black dotted line in each panel from left to right represents 2:1, 1:1 and 1:2 ratio respectively.

https://doi.org/10.5194/acp-2021-683
Preprint. Discussion started: 5 October 2021

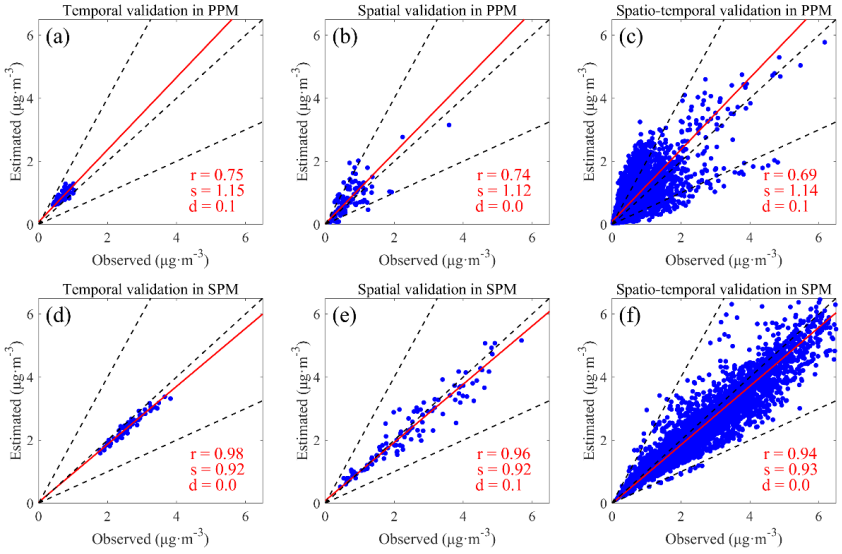

Figure 4. The scatter evaluation between the monthly mean of observed PPM(a-c)/SPM(d-f) versus that of estimated PPM/SPM in the United States. Panel (a, d), (b, e) and (c, f) denotes temporal, spatial and spatio-temporal mixed validation respectively. The red numbers in each panel indicate the Pearson correlation coefficient (r), the slope (s) and the intercept of fitting line (d). The fitting lines in red were based on the RMA regression. The black dotted line in each panel from left to right represents 2:1, 1:1 and 1:2 ratio respectively.

https://doi.org/10.5194/acp-2021-683
Preprint. Discussion started: 5 October 2021

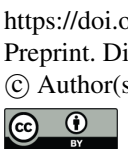

Atmospheric Chemistry and Physics Discussions

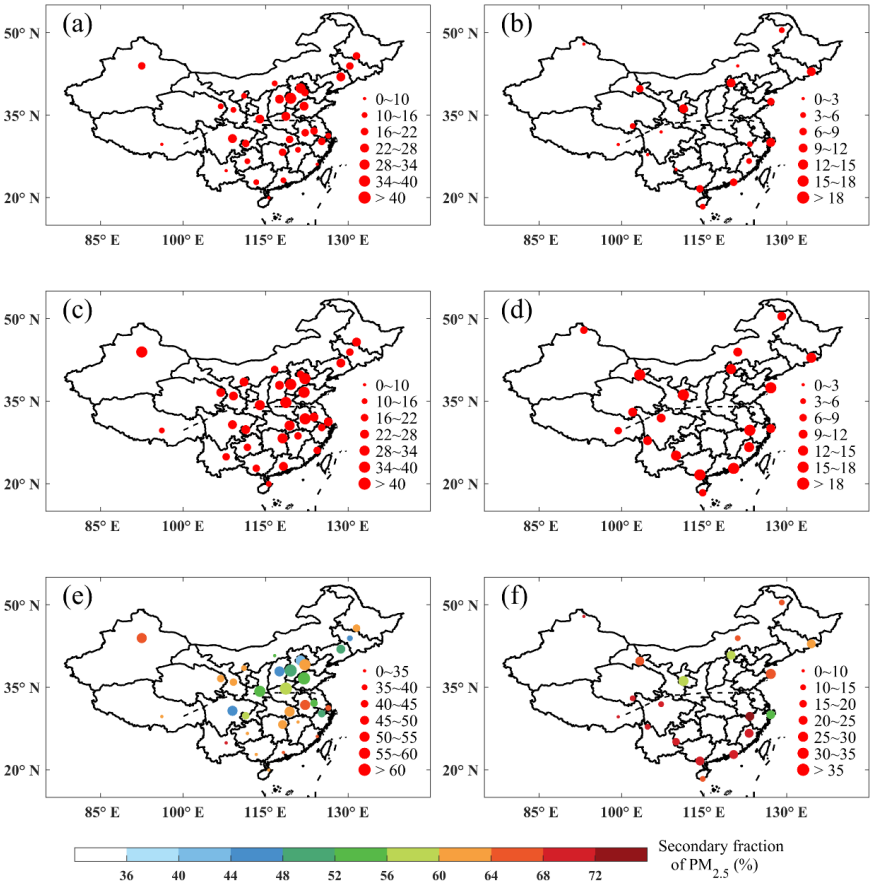

Figure 5. Spatial distributions of PPM (a, b), SPM (c, d) and total $PM_{2.5}$ concentration (e, f) averaged for the studying period. The secondary proportions of $PM_{2.5}$ (SPM/total $PM_{2.5}$) are also shown in (e, f). The left column (a, c, e) indicates populous cities. The right column (b, d, f) is for the regional background cities. The black dotted line in each panel shows the Qinling-Huaihe line.

https://doi.org/10.5194/acp-2021-683
Preprint. Discussion started: 5 October 2021

Atmospheric Chemistry and Physics Discussions

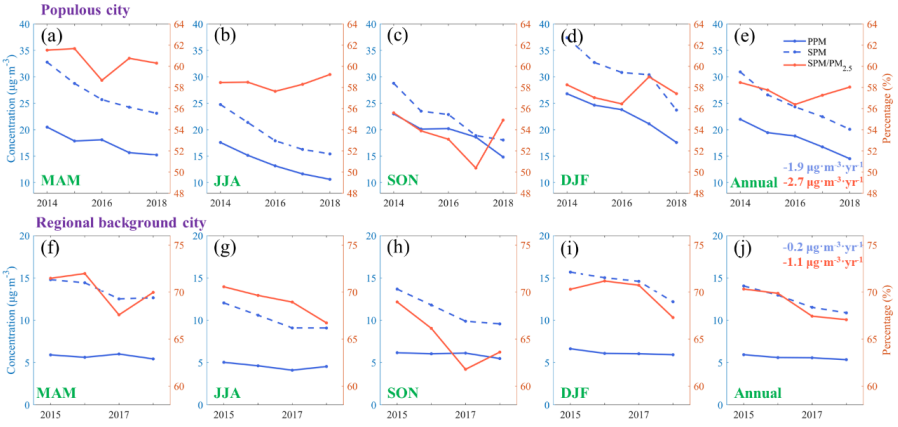

Figure 6. Inter-annual variations of PPM concentrations (blue solid line), SPM concentrations (blue dotted line) and the secondary proportions of $PM_{2.5}$ (red solid line) in populous cities (a-e) and regional background cities (f-j). MAM (a, f), JJA (b, g), SON (c, h) and DJF (d, i) denotes spring, summer, fall and winter respectively. The absolute decreases in PPM/SPM concentration are labeled in blue/red near the panel (e, j).

https://doi.org/10.5194/acp-2021-683
Preprint. Discussion started: 5 October 2021

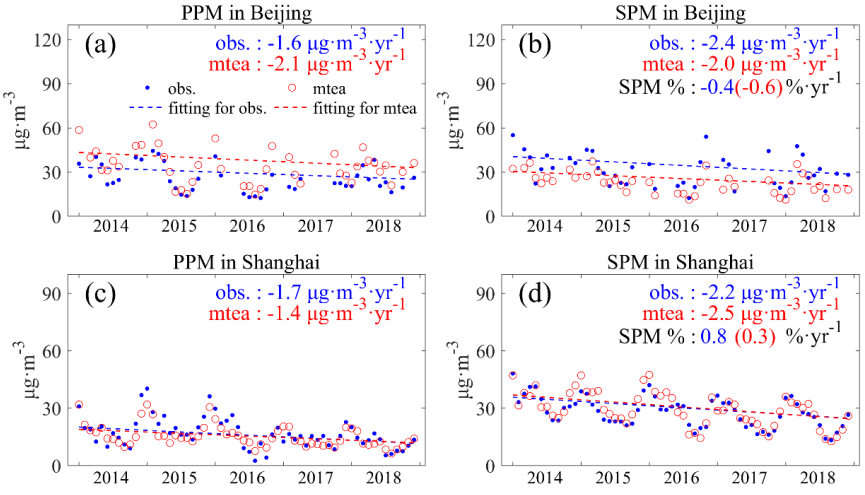

Figure 7. The monthly time series variation of PM in Beijing (a-b) and Shanghai (c-d). Panel (a, d), (b, e) denotes PPM, SPM respectively. In each panel, in-situ observation and MTEA estimation is shown in blue and red dots. Meanwhile, bule and red dotted line stands for the long-term trend in concentration changes. The values of the decrease rates in PPM and SPM concentrations as well as the relative changes in the secondary proportions of $PM_{2.5}$ (SPM %) are also provided at the upper right corner of each panel.

https://doi.org/10.5194/acp-2021-683
Preprint. Discussion started: 5 October 2021

Atmospheric Chemistry and Physics Discussions

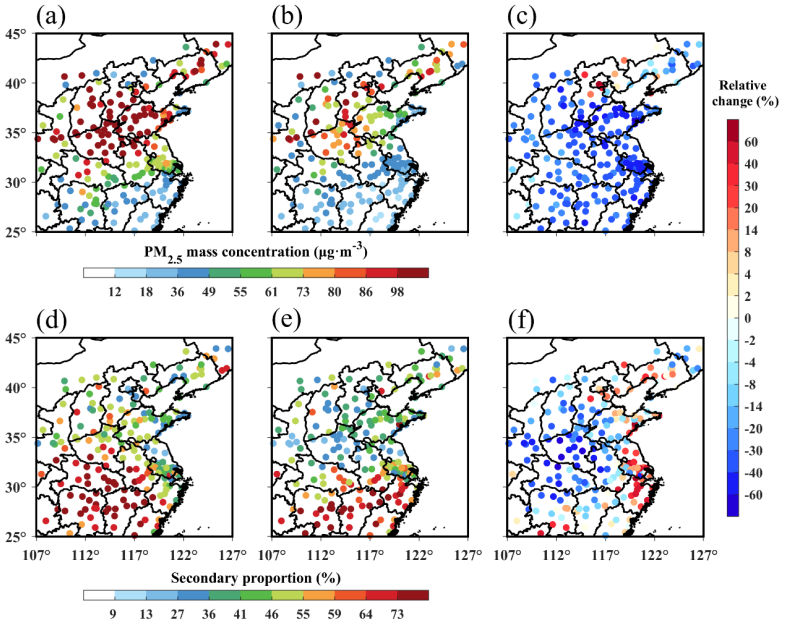

Figure 8. The application of M-TEA in estimating PPM/SPM during the COVID-19 lockdown. Panel a and b denotes the spatial distribution of $PM_{2.5}$ mass concentration before the national lockdown (01~23 Jan 2020, pre-lockdown) and during the national lockdown (23-Jan ~ 17-Feb 2020, post-lockdown). And panel c indicates the relative change between panel a and panel b, i.e. (post-lockdown – pre-lockdown)/pre-lockdown. Panel (d-f) is the same as panel (a-c), but for the secondary proportions of $PM_{2.5}$.

https://doi.org/10.5194/acp-2021-683
Preprint. Discussion started: 5 October 2021

Atmospheric Chemistry and Physics Discussions

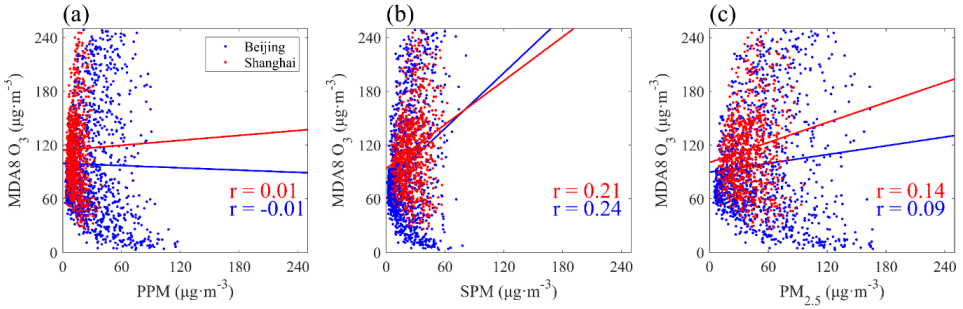

Figure 9. Scatter plot about the correlation between daily PM concentration and MDA8 O_3 concentration in Beijing (blue) and Shanghai (red). Based on the reanalysis dataset ERA5 from ECMWF, those days when precipitation took place were removed. Panel a-c indicates PPM, SPM and total $PM_{2.5}$ respectively. In each panel, solid-colored lines represent the fitting line based on Least Squares method. The Peason correlation coefficient (r) are also given at the bottom right of the panels.